Isolated fourfold fermion in BiTeI

A. Kuibarov,[1,*] A. Fedorov,[1,2,3] V. Bezguba,[1,4] H. Berger,[5] A. Yaresko,[6] V. Voroshnin,[2] A. Kordyuk,[4] P. Baumgärtel,[2] B. Büchner,[1,7] and S. Borisenko[1]

[1]*Leibniz Institute for Solid State and Materials Research, IFW Dresden, 01069 Dresden, Germany*
[2]*Helmholtz-Zentrum Berlin für Materialien und Energie, BESSY II, 12489 Berlin, Germany*
[3]*Joint Lab Functional Quantum Materials at BESSY II, 12489 Berlin, Germany*
[4]*Kyiv Academic University, 03142, Kyiv, Ukraine*
[5]*Institute of Condensed Matter Physics, Ecole Polytechnique Fédérale de Lausanne, CH-1015 Lausanne, Switzerland*
[6]*Max Planck Institute for Solid State Research, 70569 Stuttgart, Germany*
[7]*Institute for Solid State and Materials Physics, TU Dresden, 01062 Dresden, Germany*

(Received 18 February 2022; accepted 25 May 2022; published 13 June 2022)

We use angle-resolved photoemission spectroscopy to revisit the electronic structure of BiTeI, previously identified as a polar semiconductor with giant bulk Rashba splitting. We propose an alternative description, which is based on the experimentally determined crystal structure and agrees well with resistivity, quantum oscillations,and optical measurements. BiTeI emerges as a topological 3D Dirac semimetal hosting only two, well isolated from each other and rest of the band structure, Dirac points. Properly doped bulk material or the controlled synthesis of iodine-terminated surface of the pristine material promise to become a canonical condensed matter system whose physical properties are completely defined by the behavior of fourfold fermions.

DOI: 10.1103/PhysRevB.105.235112

I. INTRODUCTION

A large number of topologically nontrivial band structures continue to be discovered theoretically and experimentally, perhaps weekly. Almost all of them have very limited practical use, mainly because of two fundamental problems: the presence of other, trivial electronic states at the Fermi level and the distance of the topological features from this level. While the former requires sophisticated, so far almost unrealistic, band engineering, the latter seems to be relatively easy to overcome by doping the system with additional charge carriers. However, even shifting the Fermi level in, e.g., "minimal" topological semimetals Cd_3As_2 [1] and $TaIrTe_4$ [2] with only a few Dirac or Weyl points to match their energy location is quite challenging and remains unsuccessful. Therefore, it is important to find a system where the topological features are isolated from the trivial ones and their energy position can be easily manipulated.

BiTeI is one of the stable materials where the charge carriers concentration can be varied by doping of different atoms and which came to the focus of the research after a strong Rashba-like spin splitting of the bulk bands has been observed experimentally by ARPES [3]. Large spin-orbit splitting in the bulk is a requisite for a number of magnetotransport and optical effects including magnetic field generation by spin current [4], generation of spin current itself [5], or even noncentrosymmetric superconductivity [6]. Since then BiTeI has been intensely studied by various techniques including optical spectroscopy [7–10], ARPES [3,11–14], and quantum oscillations [8,15,16]. Ambipolar conduction [12], enhanced infrared magneto-optical response [17], orbital textures [14], as well as signatures of pressure-induced quantum phase transition [10,18,19] have been found in this material during the next couple of years, accompanied by the theoretical studies [20–23]. In spite of this attention, the fermiology of BiTeI remains controversial. Photoemission study using higher photon energies [11] found that the Rashba-like crossing parabolic dispersions seen in Ref. [3] and earlier interpreted as originating from the bulk are actually the surface states and that the true bulk states can be visible only using the higher photon energies. In contrast, Bowden *et al.* [14] observes two sets of Rashba-like dispersions persisting in a broad photon energy range and interprets them as originating from the quantum well states. The controversy as regards the origin of the Rashba-like states and corresponding Fermi surface extends to quantum oscillation experiments. While C.-R. Wang *et al.* and Bell *et al.* [15,16] find the agreement with the theoretical three-dimensional Fermi surface, although never detecting the frequency corresponding to the vertical section of the Fermi surface along c axis, Martin *et al.* [8] state that the observed oscillations support essentially two-dimensional Fermi surface. Moreover, Martin *et al.* find that the quantum oscillations originate from the bulk states, contrary to the conclusions of most of the ARPES studies.

Intriguingly, the controversy may have its roots in a tiny difference in distances between the tellurium and iodine atoms from bismuth. Despite earlier [24] and later confirmed [25] experimental results on the crystal structure, it was the "relaxed" theoretical crystal structure proposed in the initial paper [3] that was widely accepted by the community. If the experimental Bi-Te and Bi-I distances are swapped, the band structure changes significantly and implies a small and essentially three-dimensional Fermi surface.

*a.kuibarov@ifw-dresden.de

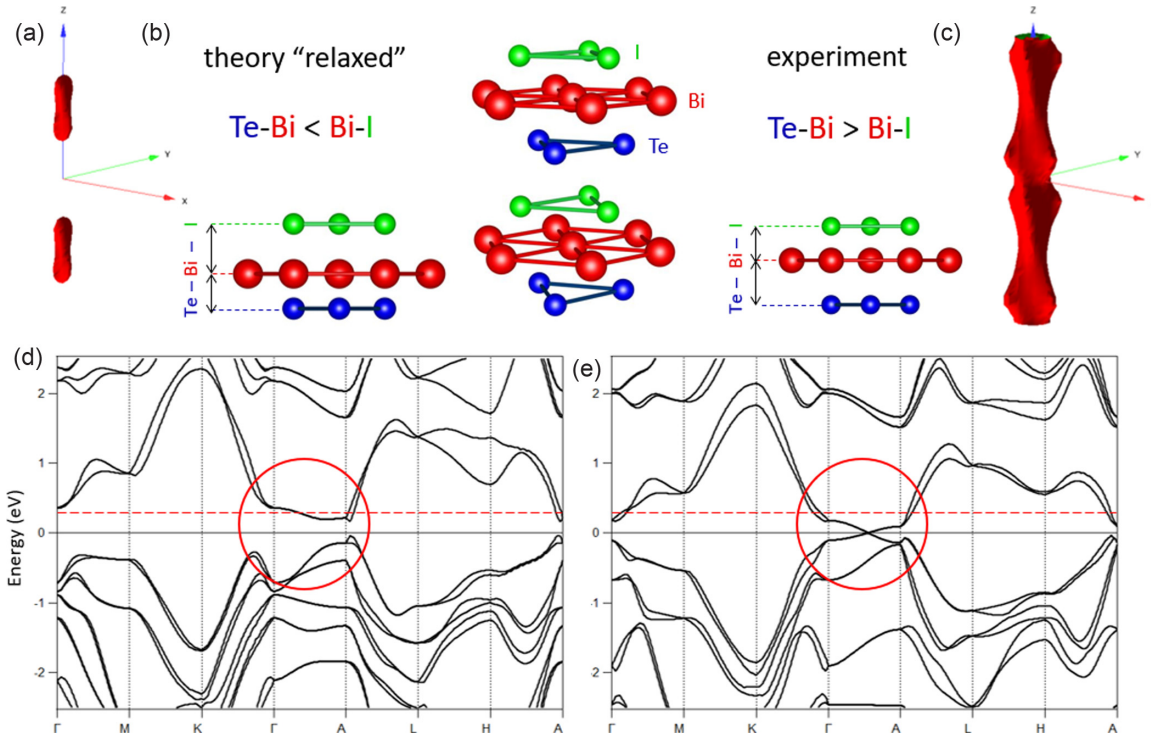

FIG. 1. Comparison of DFT calculations based on "relaxed" and experimentally determined crystal structures. (a) 3D Fermi surface implied by theoretical crystal structure of BiTeI. (b) Structural differences caused by different interatomic distances. (c) 3D Fermi surface implied by experimental crystal structure. (d) Band structure corresponding to theoretical crystal structure. Red-dashed line is the Fermi level as determined in Refs. [7,11,15,16]. (e) Band structure implied by experimental structural data. Fermi level is chosen to fit the size of the Fermi surface contours seen in the ARPES data. Red circles highlight the main difference between both types of calculations.

In the present study, we show that the band structure implied by the experiment [24,25] describes the observations by numerous techniques more consistently. BiTeI turns out to be a unique 3D Dirac semimetal with only two 3D Dirac points maximally separated in k space. Remarkably, there are no other electronic states within this 0.4-eV wide "Dirac band".

II. MATERIALS, METHODS, AND COMPUTATIONAL DETAILS

BiTeI single crystals used in experiments were grown by vapour transport method. Samples were cleaved *in situ* with pressure better than 2×10^{-10} mbar. Figures 2, 3(a), and 5 were measured at "One Squared" experimental station at BESSY synchrotron using "Scienta Omicron R4000" electron analyzer and photon energies in 15–80 eV range. Figures 3(c) and 3(e) were obtained at "U125-2 NIM" Beamline at BESSY synchrotron using "Fermiologics FeSuMa 1.0" [26] electron analyzer with photon energies 20–24 eV. Measurements in Fig. 4 were performed at IFW Dresden US-ARPES laboratory with 6-eV laser using "Scienta Omicron R4000" electron analyzer. Angular resolution of both analyzers is 0.2°.

Self-consistent band structure calculations were performed using crystal structures from [24] for experimental crystal lattice [Fig. 1(e)] and [20] for "relaxed" crystal lattice [Fig. 1(d)] using the linear muffin-tin orbital (LMTO) method in the atomic sphere approximation (ASA) as implemented in PY LMTO computer code. The Perdew-Wang parametrization [27] was used to construct the exchange correlation potential in the local density approximation (LDA). Spinorbit coupling was taken into account by solving the Dirac equation inside atomic spheres.

III. RESULTS AND DISCUSSION

In Fig. 1 we show the differences between the crystal structures, band structures, and Fermi surfaces caused by an alternative theoretical description based on relaxed atomic positions suggested earlier [3]. By now-generally accepted picture implies that contrary to the experimental data, the distance between the bismuth and iodine layers should be larger than the one between the bismuth and tellurium layers (Bi-I > Bi-Te). This change opens the energy gap turning the material from a 3D Dirac semimetal to a semiconductor and significantly alters the shape and dimensionality of the Fermi surface. The latter becomes essentially three-dimensional and consists of two separated "beans". As is seen from comparison of the near-E_F band structures highlighted by the red circles in Figs. 1(d) and 1(e) this occurred because of different behavior of the bands along the ΓA direction. Moreover, taking into account the positions of the Fermi level, set to match the size of the Fermi surface seen in ARPES, the number of charge carriers implied by theory-based crystal structure is significantly reduced. Intriguingly, the Hall coefficient data, which would clarify discrepancy from this point of view, are apparently absent in the literature.

Before we start presenting new ARPES data, which will allow us to identify which version of the band structure from

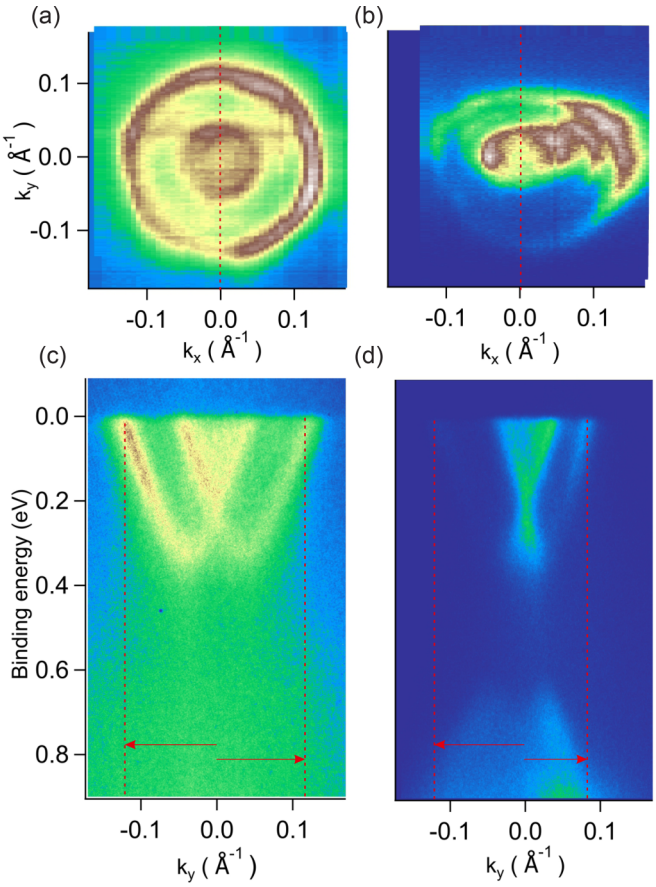

FIG. 2. Fermi surface maps of BiTeI measured at 15 K using (a) 25 eV and (b) 15 eV photon energies. [(c),(d)] Corresponding energy momentum intensity plots taken along red-dashed lines in (a) and (b), respectively. Red-dashed lines and solid arrows are used to emphasize asymmetry in ARPES spectra.

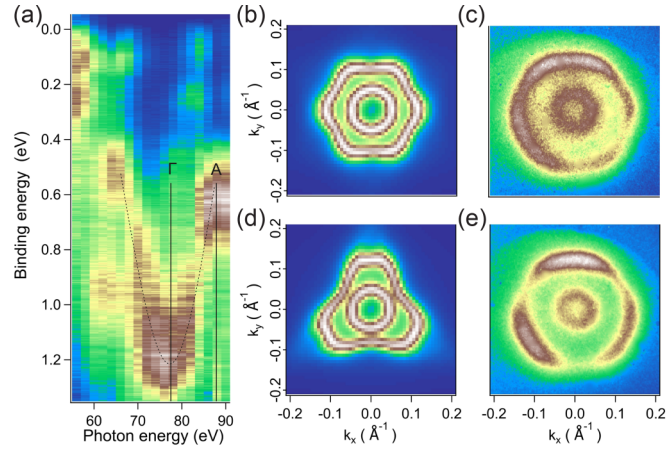

FIG. 3. (a) Photon energy scan at normal emission. Dashed curve represents valence band (VB) dispersion. Black-solid lines represents Γ and A points. Calculated maps [(b),(d)] are the FS contours implied by Fig. 1(e), blurred with the Gaussian and shown in the same color scale to simulate the photoemission data. Experimental Fermi surface maps measured with (c) 22 eV (Γ point) and (e) 24 eV photon energies using FeSuMa electron analyzer. Photon energy range 22–24 eV is approximately 10% of Γ-A distance in k space.

Fig. 1 corresponds to BiTeI, we mention that previous ARPES studies identified two terminations of the surface of BiTeI. These are not expected to be observed from the same cleave if the crystal is ideal, but with the presence of the stacking faults [12,13] their existence can be understood. In any case, since the iodine-terminated surface appears to be hole-reach thus leaving the Rashba-like states unoccupied, less stable and is subjected to ageing [13], we carried out our experiments trying to pick up the signal from the Te-terminated parts.

In Fig. 2(a) we show a Fermi surface map taken using 25 eV photons. In this case the FS contours look conventional, consisting of two, mostly circular but with some hexagonal warping, features, as in the previous ARPES studies [3,11–14]. These FS contours alone are not sufficient to distinguish between two cases since both FS [Figs. 1(a) and 1(c)] have similar horizontal sections in high-symmetry points, A and Γ/A, respectively. We note, that upon closer consideration, the map in Fig. 2(a) does contain remnants of the feature in between small and large FS and the smaller one looks broader, possibly because of small additional splitting. This is not expected in the case of theoretical 3D-Fermi surface [Fig. 1(a)]. The only occupied flat portion of the band along ΓA-direction near A point [Fig. 1(d)] implies only one set of Fermi surface contours in ARPES maps because of moderate k_z resolution of the method, which implies an integration of the band structure over significant part of perpendicular momentum. In contrast, two flat portions of the bands along ΓA in the experimental band structure [Fig. 1(e)] fully agree with the presence of two sets of the FS contours in the integrated along k_z spectrum. We also note a light asymmetry of the underlying dispersion with respect to the zeroth momentum along k_y direction shown in Fig. 1(c). This is not surprising, since the trigonal warping is naturally present in a material with no inversion symmetry.

According to the calculations, the 3D FS from Fig. 1(c) should have more such 180° asymmetric sections then the one implied by the "relaxed" model. In Fig. 2(b) we present the FS map, which corresponds perhaps to the maximum distortion of this kind. Recorded with 15 eV photons, this map does deviate from the one from Fig. 2(a) and, actually, from all ARPES data published earlier. We stress that although the most of the asymmetry of the map comes from the strong suppression of the intensity at negative k_y due to matrix element effects, there is a clear evidence for the asymmetry of the peaks of the spectral function. Trigonally warped FS contours are supported by clearly asymmetric dispersion seen in Fig. 2(d). This dataset rules out any artificial asymmetry of the FS maps, which may be caused by rotating the sample or scanning the signal electronically through the entrance slit of conventional hemispherical analyzer. The Fig. 2(d) represents an energy-momentum distribution taken along the entrance slit while keeping all other experimental parameters fixed. Such a modification of the 2D section of the FS clearly speaks in favour of bulk origin of the detected electronic states and cannot be explained either by surface contribution or quantum well states. In order to bring photon energies and k_z scale in correspondence, we recorded the normal emission spectra as a function of $h\nu$ [Fig. 3(a)]. Comparing the data to the band structures from Figs. 1(d) and 1(e) one can unambiguously identify the band dispersing by approximately 0.7 eV

from Γ to A immediately below the bands forming the 3D Dirac point. We note, that "relaxed" band structure implies *two* features in this region, not observed experimentally. The behavior of all valence bands near the A point in the binding energy range down to 5 eV also shows much better agreement with our scenario (see Fig. S1 in the Supplemental Material [28]). Now we can estimate the inner potential ($V_0 = 11$) in the free-electron approximation and identify photon energies corresponding to the high symmetry points along k_z using $k_z = 0.512\sqrt{(E_k + V_0)}$, where E_k is electron kinetic energy. With this information we can now sample the 3D Fermi surface in that portion of BZ along k_z, which will allow us to distinguish between two scenarios. We also switch to another way of detecting the photoelectrons, namely to the technology [26] that allows the Fermi surface map to be detected at once without rotating the sample or scanning the electron beam. This approach minimizes the influence of the matrix elements by keeping the geometry of the experiment constant and enables isotropic momentum resolution. In Figs. 3(b) and 3(c) we compare the calculated FS cross section going through the Γ point with the FS map taken at 22 eV. Apart from the slight differences in size, the agreement is remarkable—the sharp and clearly resolved features with symmetric and hexagonal shapes are fully reproduced. This is in sharp contrast to the "relaxed" calculations [Fig. 1(a)], which predict no FS at Γ and therefore only blurred contributions from other k_zs are expected in ARPES due to the moderate resolution along this direction. The model based on experimental crystal structure also implies that going away from Γ point towards A point the FS section should become strongly trigonally warped. Also this observation is clearly supported by the ARPES data. In Figs. 3(d) and 3(e) we show the corresponding results, which again are in a full qualitative agreement. We emphasize that using the new technology the intensity distribution is minimally influenced by the experimental geometry, free from stripes due to scanning, and thus reproduces spectral function more precisely.

We have also performed experiments using a 6-eV laser. According to the universal curve, the escape depth of the photoelectrons in this case is larger than in any previous ARPES study of BiTeI, and the spectra are therefore most representative of the bulk. In addition, the ultimate momentum resolution along k_x and k_y enables exact alignment of the sample and identification of all features. Such low photon energy also means that k_z resolution becomes worse and the radius of the sphere in k space probed by ARPES is minimal. Both factors lead to integration of the signal along k_z. Nevertheless, the result presented in Fig. 4 exactly corresponds to our scenario and contradicts the "relaxed" model as well as interpretations in terms of the surface states—both sets of parabolic features suggested by Fig. 1(e) are present and thus are of bulk origin. Remarkably, these two sets of Rashba-like split parabolas are observed now in a very broad photon energy range, where the resolution is sufficient to detect them: from 6 eV here via 22–70 eV interval in Ref. [14] up to 93 eV in e.g., Ref. [12] (Fig. S3). There was no evidence for the breaks implied by essentially 3D FS [Fig. 1(a)] in this photon energy range.

Finally, we try to locate the 3D Dirac points implied by our description of BiTeI directly. The Fig. 5(a) shows a Dirac point in momentum-energy cut taken using 64 eV photons. It

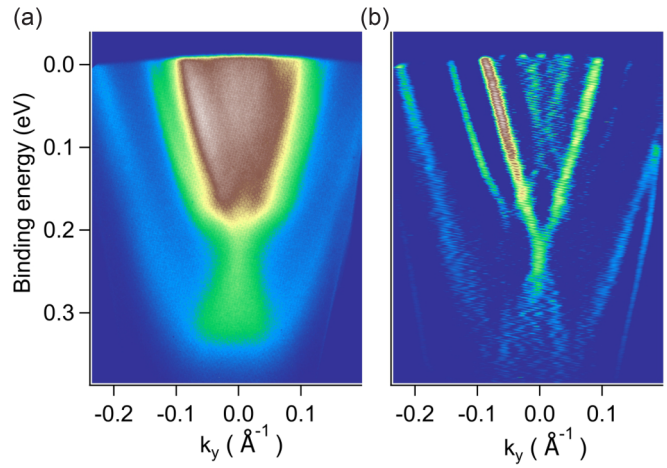

FIG. 4. (a) Photoemission intensity plot measured at 3.2 K with 6 eV laser and (b) corresponding second derivative plot.

is seen at approximately 0.48 eV binding energy as a typical crossing of two dispersing features. As expected for such binding energies, this crossing appears blurred due to the increased scattering. Tuning the photon energy away from this k_z towards the Γ point, we observe no evidence for the crossing at 74 eV photon energies in Fig. 5(b) in a full agreement

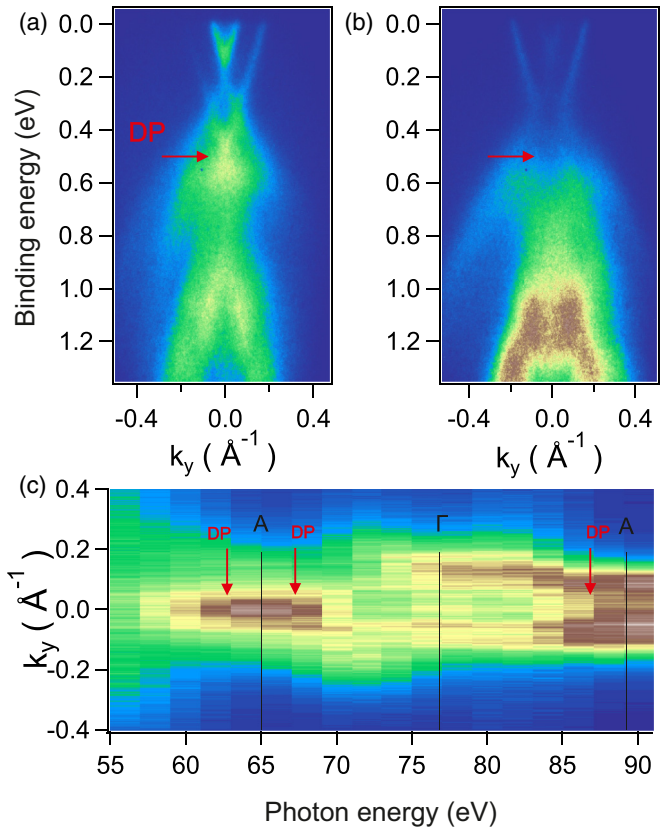

FIG. 5. Photoemission intensity plot obtained at 15 K by using (a) 66 eV and (b) 74 eV photon energies. Red arrows show the position of Dirac point. (c) Constant energy ARPES momentum distribution curve (0.48 ± 0.01 eV binding energies) as a function of photon energy.

with the 3D electronic structure implied by Fig. 1(e). We also present an attempt to find more Dirac points in momentum space considering in Fig. 5(c) a map of intensity in (k_z, k_y) plane corresponding to the determined above energy of Dirac crossing (0.48 eV). Band structure in Fig. 1(e) implies pairs of 3D Dirac points centered at A points when going along k_z since the crossing is closer to A point than to Γ point. In qualitative agreement with this expectation we do observe the localization of intensity near A points. However, experiment shows that shift of Dirac points towards A point is even larger since two Dirac points are not seen split near A points resulting in the elongated along k_z intensity maxima.

Our ARPES results prove that BiTeI is not a semiconductor as previously thought, but rather a 3D Dirac semimetal with a unique isolation of two Dirac points from the rest of the band structure features, both in terms of energy and momentum. Its quasi-two-dimensional Fermi surface [Fig. 1(c)] is in an excellent agreement with resistivity measurements [3] and all quantum oscillation studies [8,15,16], which never detected a frequency corresponding to the orbits in (k_z, k_x/k_y) planes. As our calculations of the optical response show (Fig. S2 in the Supplemental Material [28]), it is hard to distinguish between two scenarios when Fermi level is shifted by ∼300 meV, as in the experiment. This makes all previous arguments in favour of agreement between the optics and ARPES valid also for our scenario for the pristine samples. However, the sharpness of the edge in optical conductivity for BiTeI with lower carriers concentration, as, e.g., in Fig. 2 of Ref. [7], show better agreement with the calculations corresponding to the experimental crystal structure Fig. S2 (in the Supplemental Material [28]).

Having an ideal 3D Dirac semimetal with isolated Dirac points at the Fermi level would help to single out the physical properties caused exactly by fourfold fermions. Electronic structure of BiTeI seems to be unique since despite inversion symmetry is broken and the spin-orbit coupling for Te p(0.6 eV), I p(0.8 eV), and Bi p(2.3 eV) states is very strong, being comparable to their band widths, this does not lead to lifting the fourfold degeneracy of the Dirac point. This degeneracy is symmetry protected because the wave functions of the two pairs of bands forming the fourfold Dirac point transform according to different two-dimensional irreducible representations of the double group C_{4v}, which is the group of a wave vector along the Γ-A line. Up to now numerous theoretical studies predicted exotic physical properties but it was not possible to bring isolated 3D Dirac points to the Fermi level experimentally. A straightforward way would be to dope the system with holes, but usually such approaches are not successful. Our study of Te-terminated surface as well as previous ARPES and STM studies [12,13,29] of I-terminated surface imply that the latter is already very close to that ideal 3D Dirac semimetal state. If the typical size of natural iodine termination is of the order of 100 nm size, it may become possible to stabilize and increase this area, so that devices can be built enabling a broad spectrum of experiments highlighting BiTeI from its new, different side.

ACKNOWLEDGMENTS

We acknowledge the support from SFB 1143 "Correlated Magnetism" and Würzburg-Dresden Cluster of Excellence on Complexity and Topology in Quantum Matter - ct.qmat. A.K., V.B., A.K., and S.B. have been supported by UKRATOP project. We thank the Helmholtz-Zentrum Berlin für Materialien und Energie for the allocation of synchrotron radiation beamtime.

[1] S. Borisenko, Q. Gibson, D. Evtushinsky, V. Zabolotnyy, B. Büchner, and R. J. Cava, Experimental Realization of a Three-Dimensional Dirac Semimetal, Phys. Rev. Lett. **113**, 027603 (2014).

[2] E. Haubold, K. Koepernik, D. Efremov, S. Khim, A. Fedorov, Y. Kushnirenko, J. van den Brink, S. Wurmehl, B. Büchner, T. K. Kim, M. Hoesch, K. Sumida, K. Taguchi, T. Yoshikawa, A. Kimura, T. Okuda, and S. V. Borisenko, Experimental realization of type-II Weyl state in noncentrosymmetric $TaIrTe_4$, Phys. Rev. B **95**, 241108(R) (2017).

[3] K. Ishizaka, M. S. Bahramy, H. Murakawa, M. Sakano, and T. Shimojima, Giant Rashba-type spin splitting in bulk BiTeI, Nat. Mater. **10**, 521 (2011).

[4] I. Mihai Miron, G. Gaudin, S. Auffret, B. Rodmacq, A. Schuhl, S. Pizzini, J. Vogel, and P. Gambardella, Current-driven spin torque induced by the Rashba effect in a ferromagnetic metal layer, Nat. Mater. **9**, 230 (2010).

[5] Z. Liu, S. Thirupathaiah, A. N. Yaresko, S. Kushwaha, Q. Gibson, W. Xia, Y. Guo, D. Shen, R. J. Cava, and S. V. Borisenko, A giant bulk-type Dresselhaus splitting with 3d chiral spin texture in IrBiSe, Phys. Status Solidi RRL **14**, 1900684 (2020).

[6] E. Bauer, G. Hilscher, H. Michor, C. Paul, E. W. Scheidt, A. Gribanov, Y. Seropegin, H. Noël, M. Sigrist, and P. Rogl, Heavy Fermion Superconductivity and Magnetic Order in Noncentrosymmetric $CePt_3Si$, Phys. Rev. Lett. **92**, 027003 (2004).

[7] J. S. Lee, G. A. H. Schober, M. S. Bahramy, H. Murakawa, Y. Onose, R. Arita, N. Nagaosa, and Y. Tokura, Optical Response of Relativistic Electrons in the Polar BiTeI Semiconductor, Phys. Rev. Lett. **107**, 117401 (2011).

[8] C. Martin, E. D. Mun, H. Berger, V. S. Zapf, and D. B. Tanner, Quantum oscillations and optical conductivity in Rashba spin-splitting BiTeI, Phys. Rev. B **87**, 041104(R) (2013).

[9] A. A. Makhnev, L. V. Nomerovannaya, T. V. Kuznetsova, O. E. Tereshchenko, and K. A. Kokh, Optical properties of BiTeI semiconductor with a strong Rashba spin-orbit interaction, Opt. Spectrosc. **117**, 764 (2014).

[10] M. K. Tran, J. Levallois, P. Lerch, J. Teyssier, A. B. Kuzmenko, G. Autès, O. V. Yazyev, A. Ubaldini, E. Giannini, D. van der Marel, and A. Akrap, Infrared- and Raman-Spectroscopy Measurements of a Transition in the Crystal Structure and a Closing of the Energy Gap of BiTeI under Pressure, Phys. Rev. Lett. **112**, 047402 (2014).

[11] G. Landolt, S. V. Eremeev, Y. M. Koroteev, B. Slomski, S. Muff, T. Neupert, M. Kobayashi, V. N. Strocov, T. Schmitt, Z. S. Aliev, M. B. Babanly, I. R. Amiraslanov, E. V. Chulkov, J. Osterwalder, and J. H. Dil, Disentanglement of Surface and

Bulk Rashba Spin Splittings in Noncentrosymmetric BiTeI, Phys. Rev. Lett. **109**, 116403 (2012).

[12] A. Crepaldi, L. Moreschini, G. Autès, C. Tournier-Colletta, S. Moser, N. Virk, H. Berger, P. Bugnon, Y. J. Chang, K. Kern, A. Bostwick, E. Rotenberg, O. V. Yazyev, and M. Grioni, Giant Ambipolar Rashba Effect in the Semiconductor BiTeI, Phys. Rev. Lett. **109**, 096803 (2012).

[13] S. Fiedler, L. El-Kareh, S. V. Eremeev, O. E. Tereshchenko, C. Seibel, P. Lutz, K. A. Kokh, E. V. Chulkov, T. V. Kuznetsova, V. I. Grebennikov, H. Bentmann, M. Bode, and F. Reinert, Defect and structural imperfection effects on the electronic properties of BiTeI surfaces, New J. Phys. **16**, 075013 (2014).

[14] L. Bawden, J. M. Riley, C. H. Kim, R. Sankar, E. J. Monkman, D. E. Shai, H. I. Wei, E. B. Lochocki, J. W. Wells, W. Meevasana *et al.*, Hierarchical spin-orbital polarization of a giant Rashba system, Sci. Adv. **1**, e1500495 (2015).

[15] C.-R. Wang, J.-C. Tung, R. Sankar, C.-T. Hsieh, Y.-Y. Chien, G.-Y. Guo, F. C. Chou, and W.-L. Lee, Magnetotransport in copper-doped noncentrosymmetric BiTeI, Phys. Rev. B **88**, 081104(R) (2013).

[16] C. Bell, M. S. Bahramy, H. Murakawa, J. G. Checkelsky, R. Arita, Y. Kaneko, Y. Onose, M. Tokunaga, Y. Kohama, N. Nagaosa, Y. Tokura, and H. Y. Hwang, Shubnikov–de Haas oscillations in the bulk Rashba semiconductor BiTeI, Phys. Rev. B **87**, 081109(R) (2013).

[17] L. Demkó, G. A. H. Schober, V. Kocsis, M. S. Bahramy, H. Murakawa, J. S. Lee, I. Kézsmárki, R. Arita, N. Nagaosa, and Y. Tokura, Enhanced Infrared Magneto-Optical Response of the Nonmagnetic Semiconductor BiTeI Driven by Bulk Rashba Splitting, Phys. Rev. Lett. **109**, 167401 (2012).

[18] X. Xi, C. Ma, Z. Liu, Z. Chen, W. Ku, H. Berger, C. Martin, D. B. Tanner, and G. L. Carr, Signatures of a Pressure-Induced Topological Quantum Phase Transition in BiTeI, Phys. Rev. Lett. **111**, 155701 (2013).

[19] J. Park, K.-H. Jin, Y. J. Jo, E. S. Choi, W. Kang, E. Kampert, J.-S. Rhyee, S.-H. Jhi, and J. S. Kim, Quantum oscillation signatures of pressure-induced topological phase transition in BiTeI, Sci. Rep. **5**, 15973 (2015).

[20] M. S. Bahramy, R. Arita, and N. Nagaosa, Origin of giant bulk Rashba splitting: Application to BiTeI, Phys. Rev. B **84**, 041202(R) (2011).

[21] G. A. H. Schober, H. Murakawa, M. S. Bahramy, R. Arita, Y. Kaneko, Y. Tokura, and N. Nagaosa, Mechanisms of Enhanced Orbital Dia- and Paramagnetism: Application to the Rashba Semiconductor BiTeI, Phys. Rev. Lett. **108**, 247208 (2012).

[22] M. S. Bahramy, B.-J. Yang, R. Arita, and N. Nagaosa, Emergence of non-centrosymmetric topological insulating phase in BiTeI under pressure, Nat. Commun. **3**, 679 (2012).

[23] S. Schwalbe, R. Wirnata, R. Starke, G. A. H. Schober, and J. Kortus, *Ab initio* electronic structure and optical conductivity of bismuth tellurohalides, Phys. Rev. B **94**, 205130 (2016).

[24] A. V. Shevelkov, E. V. Dikarev, R. V. Shapanchenko, and B. A. Popovkin, Crystal structures of bismuth tellurohalides BieX (X = Cl, Br, I) from x-ray powder diffraction data J. Solid State Chem. **114**, 379 (1995).

[25] V. A. Kulbachinskii, V. G. Kytin, A. A. Kudryashov, A. N. Kuznetsov, and A. V. Shevelkov, On the electronic structure and thermoelectric properties of BiTeBr and BiTeI single crystals and of BiTeI with the addition of BiI_3 and CuI, J. Solid State Chem. **193**, 154 (2012).

[26] S. Borisenko, A. Fedorov, A. Kuibarov, M. Bianchi, V. Bezguba, P. Majchrzak, P. Hofmann, P. Baumgärtel, V. Voroshnin, Y. Kushnirenko *et al.*, Fermi surface tomography, arXiv:2105.15055

[27] J. P. Perdew and Y. Wang, Accurate and simple analytic representation of the electron-gas correlation energy, Phys. Rev. B **45**, 13244 (1992).

[28] See Supplemental Material at http://link.aps.org/supplemental/10.1103/PhysRevB.105.235112 for the calculations of optical conductivity, a detailed comparison of electron dispersion for both crystal structures and additional ARPES data regarding surface state question in BiTeI.

[29] C. J. Butler, H.-H. Yang, J.-Y. Hong, S.-H. Hsu, R. Sankar, C.-I. Lu, H.-Y. Lu, K.-H. O. Yang, H.-W. Shiu, C.-H. Chen, C.-C. Kaun, G.-J. Shu, F.-C. Chou, and M.-T. Lin, Mapping polarization induced surface band bending on the Rashba semiconductor BiTeI, Nat. Commun. **5**, 4066 (2014).